Experimental ARoF System Based on OPLL Mm-Wave Generation for Beyond 5G

Experimental ARoF System Based on OPLL Mm-Wave Generation for Beyond 5G

Javier Pérez Santacruz[1], Delphin Dodane[2], Jerome Bourderionnet[2], Simon Rommel[1], Antonio Jurado-Navas[3], Ulf Johannsen[1], and Idelfonso Tafur Monroy[1]

[1] *Institute for Photonic Integration (IPI), Eindhoven University of Technology, 5600 MB Eindhoven, the Netherlands*
[2] *Thales Research & Technology, 91767 Palaiseau Cedex, France*
[3] *Department of Communications Engineering, University of Málaga, Campus de Teatinos, 29071 Málaga, Spain*
j.perez.santacruz@tue.nl

Abstract: We experimentally analyze the ARoF based on OPLL mm-Wave generation performance for 5G fronthaul. Remarkable performance improvements are achieved for all 5G NR numerologies and different OPLL configurations despite their inherently high phase noise level.

OCIS codes: (060.5625) Radio frequency photonics; (060.4510) Optical communications.

1. Introduction

The fifth-generation (5G) of mobile networks aims to satisfy the upcoming applications demands. 5G new radio (NR) will bring a large enhancement in terms of data rate and latency among others. Exploiting the millimeter-Wave (mm-Wave) domain is required to achieve the 5G data rate goals. However, since mm-Wave signals present high free-space path loss (FSPL), the number of mm-Wave remote units (RUs) will be much larger than in the current mobile network. Then, analog radio-over-fiber (ARoF) technology arises as an adequate solution for the beyond 5G fronthaul since it offers interesting benefits such as low latency, low complex RUs, and efficient spectrum usage [1,2]. Hence, ARoF enables a scalable deployment of the mm-Wave RUs for the future 5G architecture.

The optical mm-Wave generation is key to achieve a stable ARoF communication (see Fig. 1 (a)), with external modulation and optical phase locked loop (OPLL) being two of the most popular techniques (see their schematics in Fig. 1 (b)). Since external modulation technique uses the high order harmonics produced by applying the RF source to the modulator, the generation of the two-tone suffers high attenuation [3]. On the other hand, OPLL technique presents better performance in terms of power efficiency. Nevertheless, OPLL implies higher phase noise level (see Fig. 1 (c)).

Orthogonal frequency division multiplexing (OFDM) is the standardized 5G waveform by 3rd Generation Partnership Project (3GPP) [4]. However, phase noise is one of the major limiting factors in OFDM mm-Wave ARoF systems because of the low subcarrier spacing utilized in 5G [5]. Therefore, 5G ARoF systems based on OPLL mm-Wave generation have to implement phase noise compensation in the receiver and, thus, the benefits of employing OPLL technique, as the power efficiency, can be taken. In this paper, we present an experimental ARoF setup up based on OPLL mm-Wave generation. Different OPLL configurations and all 5G NR numerologies are tested in this setup. The experimental results achieve the 5G requirements for both 16-quadrature amplitude modulation (16-QAM) and 64-QAM. Hence, the viability of employing power efficient ARoF systems based on OPLL for the beyond 5G infrastructure is demonstrated.

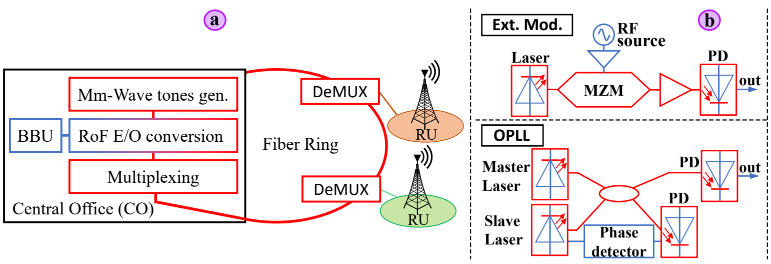

c

	Ext. Mod.	OPLL
Phase noise	Low	Medium
Induced power fading	Yes*	No
Power consumption	High	Medium
Cost	Medium	Medium
Linear response	No	Yes

* Can be solved by splitting the two tones and, then, modulating one of them with the data signal (it requires more complexity).

Fig. 1. (a) ARoF fronthaul for beyond 5G. (b) External modulation and OPLL schemes. (c) Comparative table between external modulation and OPLL techniques. BBU: base band unit, DeMUX: demultiplexer.

2. Experimental testbed

Figure 2 (a) shows the experimental setup employed in this work. First, two distributed feedback lasers (DFB), operating at C-band, generate two optical carriers with a separation of 24.75 GHz (K-band). DFB 1 and DFB 2 constitute the master and slave lasers, respectively. Next, the generated tones are combined by a 50/50 optical coupler. One of the outputs of the coupler is employed to track the phase difference between the two tones. For that, the mm-Wave carrier output is generated from the beat signal formed between the two tones, which is detected by a photodiode (PD). Then, the resulting signal is boosted and its phase is compared to the reference signal from a local oscillator (LO) using an RF mixer. The phase error signal is introduced in the RF loop filter (LF) and is used to adjust the frequency of the slave laser, forcing it to track the master laser [3]. Hence, the phase difference between the two lasers is adjusted, producing optical tones more correlated, thus reducing the final phase noise of the system.

The other output of the coupler is used to modulate the two optical tones with the OFDM signal by a Mach-Zehnder modulator (MZM), biased in the quadrature point. An isolator protects the OPLL from reflections. The OFDM signal is generated by an intermediate frequency (IF) of 1 GHz with an arbitrary waveform generator (AWG) of 12.5 GSa/s. Then, the modulated optical signal beats in a second PD, producing RF sidebands at 23.75 and 25.75 GHz. Next, this RF signal is downconverted by mixing with a second LO of 23 GHz, producing a second IF of 1.75 GHz. Thereby, the RF sidebands move to 0.75 and 2.75 GHz, respectively. Last, the downconverted signal is boosted by a 22 dB RF amplifier and sampled by a digital phosphor oscilloscope (DPO) at 12.5 GSa/s.

The graph of Fig. 2 (b) illustrates the power spectral density (PSD) of the phase noise in the RF signal after the second PD for different bandwidth values of the OPLL LF. Observing Fig. 2 (b), it can be noticed that the phase noise PSD amplitude decreases as the OPLL LF bandwidth increments. However, the 700 kHz and 1000 kHz bandwidth cases depict high PSD peaks at its cut off frequencies. Thereby, it is not clear what it is the best OPLL configuration for an OFDM communication system and, then, these configurations should be compared. Furthermore, different OFDM configurations are transmitted through the setup. These OFDM configurations embrace all 5G NR numerologies (15–240 kHz) and their main parameters are presented in table of Fig. 2 (c) [4]: subcarrier spacing (Δf), total number of subcarriers (N), and cyclic prefix (CP) period (T_{cp}). Moreover, a photo of the main components of the OPLL block is shown in Fig. 2 (d).

Finally, Figs. 2 (e) and (f) show the digital signal processing (DSP) block diagrams at the transmitter and receiver sides, respectively. At the transmitter side, a classical OFDM transmitter is used and, then, an IF upconversion process is performed. At the receiver side, first, the sampled signal by the DPO is separated in two branches. The upper branch realizes a band-pass filter (BPF), maintaining the RF carrier and OFDM sidebands. In the lower branch, the RF carrier is obtained by a low-pass filter (LPF). Then, the outputs of the two branches are multiplied, moving the OFDM signal to the initial IF of 1 GHz. This technique is called RF-pilot-assisted and allows to mitigate the phase noise by using the RF tone for the downconversion process. Last, the IF downconversion, the synchronization, the carrier frequency offset (CFO) compensation, and the OFDM receiver blocks are performed.

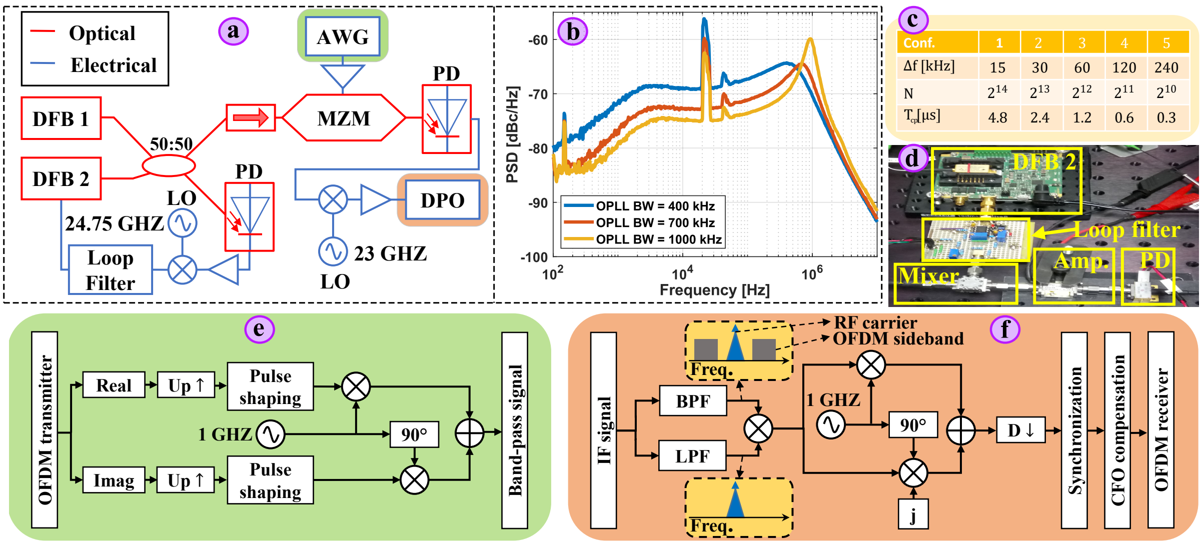

Fig. 2. Experimental testbed: (a) schematic of the setup, (b) PSD of the phase noise for different OPLL LF bandwidths, (c) table with the parameters of the used OFDM configurations, (d) transmitter DSP block diagram in the AWG, (e) and receiver DSP block diagram in the DPO.

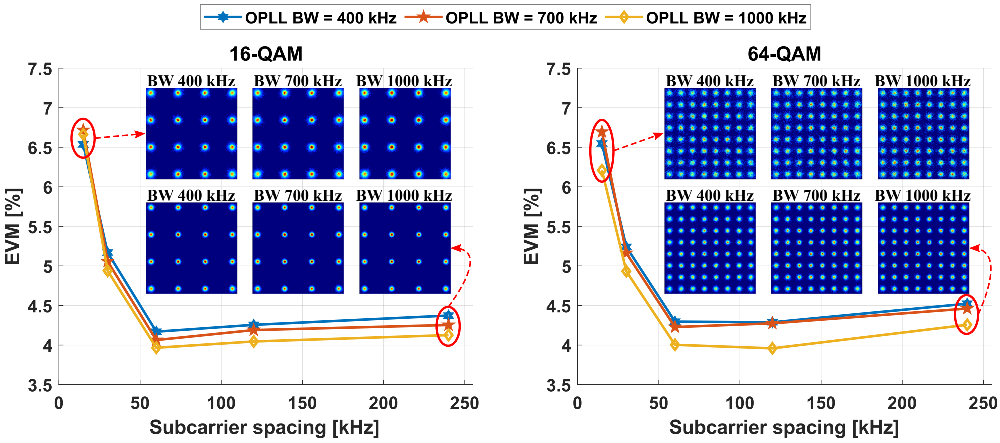

Fig. 3. EVM as a function of the subcarrier spacing for the under test OPLL configurations.

3. Experimental results and discussions

Figure 3 shows the results of the experimental setup. These results are expressed in terms of error vector magnitude (EVM) for different subcarrier spacing values and several OPLL configurations. Two modulation orders have been evaluated: 16-QAM (left graph) and 64-QAM (right graph). In both graphs, it can be noticed that EVM decreases as the subcarrier spacing value increases. This fact is because the inter-carrier interference (ICI) level induced by the phase noise is higher for lower subcarrier spacing values [2]. Furthermore, a slight increase of the EVM values is observed for larger subcarrier spacing values because the density of pilots is lower for these configurations and thus the equalization process performs worse.

Moreover, both graphs show that the OPLL configuration of 1000 kHz is the best case in terms of EVM because the used RF-pilot-assisted technique compensates the phase noise better due to the PSD shape of this OPLL configuration (see graph of Fig. 2 (b)). The EVM results are below the 5G EVM threshold: 12.5 % and 8 % for 16-QAM and 64-QAM, respectively. Thus, all the evaluated numerologies fulfill the 5G requirements. However, the subcarrier spacing configurations between 60–240 kHz exhibit better performance than the 15 and 30 kHz cases. 3GPP 5G standard recommends to employ subcarrier spacing values of 60, 120, and 240 kHz for bearer frequencies above 6 GHz [4]. Therefore, the experimental results of this work consolidate the aforementioned 5G recommendation.

4. Conclusions

An ARoF system based on OPLL K-band mm-Wave generation has been experimentally validated. Different OPLL configurations and all 5G NR numerologies have been evaluated through this setup. Moreover, the RF-pilot-assisted technique has been employed to mitigate the relatively high phase noise level originating from the OPLL technique. Our experimental results satisfy the 5G requirements for both 16-QAM and 64-QAM constellations. Thereby, the viability of using the OPLL technique for mm-Wave generation is proven in ARoF systems oriented towards 5G. Hence, this work supports ARoF as a suitable solution for the fronthaul in the 5G architecture and beyond.

Acknowledgments This work has been supported by blueSPACE (GA no. 762055) and the 5G STEP FWD (GA no. 72242) projects funded by the European Union's Horizon2020 research and innovation program.

References

1. S. Rommel *et al.*, "Towards a Scaleable 5G Fronthaul: Analog Radio-over-Fiber and Space Division Multiplexing," *J. Lightw. Technol.*, vol. 38, no. 19, pp. 5412–5422, 2020.
2. J. Perez Santacruz *et al.*, "Analysis and Compensation of Phase Noise in mm-Wave OFDM ARoF Systems for Beyond 5G," *J. Lightw. Technol.*, 2020, in press.
3. I. Degli-Eredi *et al.*, "Millimeter-wave Generation Using Hybrid Silicon Photonics," Journal of Optics, 2020, in press.
4. 3GPP, *3rd Generation Partnership Project; Technical Specification Group Radio Access Network; Study on New Radio (NR) access technology. 3GPP TR 38.912, version 16.0.0*, 2020.
5. A. Delmade *et al.*, "OFDM Baud Rate Limitations in an Optical Heterodyne Analog Fronthaul Link using Unlocked Fibre Lasers," 2019 International Topical Meeting on Microwave Photonics (MWP), Ottawa, ON, Canada, 2019.